Iterative Multisymbol Noncoherent Reception of Coded CPFSK

Matthew C. Valenti, *Senior Member, IEEE,* Shi Cheng, *Member, IEEE,* and Don Torrieri, *Senior Member, IEEE*

***Abstract*—A system involving the multisymbol noncoherent reception of coded continuous-phase frequency-shift keying is developed, optimized, and analyzed. Unlike coherent systems, the modulation index of the waveform does not need to be rational with a small denominator, and the oscillator only needs to be stable for the duration of a small block of symbols. The achievable performance over AWGN and Rayleigh block-fading channels is determined by computing the average mutual information, which is the capacity of a channel using the given modulation format and receiver architecture under the constraint of uniformly distributed input symbols. The code rate and modulation index are jointly optimized with respect to average mutual information under a bandwidth constraint. For binary and quaternary signaling, the information-theoretic results are corroborated by bit-error-rate curves generated using a standardized turbo code in conjunction with iterative demodulation and decoding. It is shown that, while more robust than a system with coherent reception, the proposed system offers superior energy efficiency compared with conventional single-symbol noncoherent reception.**

***Index Terms*—Continuous-phase modulation, noncoherent reception, channel capacity, block fading, channel coding.**

I. Introduction

CONTINUOUS-PHASE frequency-shift keying (CPFSK) is a type of full-response continuous-phase modulation (CPM) that is characterized by the use of rectangular phase-shaping functions. Like other forms of CPM, CPFSK has attractive spectral characteristics because the smooth phase transitions between adjacent symbols reduce out-of-band power. A key benefit of CPFSK is that it can be noncoherently detected, which can provide improved robustness and complexity savings relative to coherent detection. The complexity savings of noncoherent detection are due to the fact that it does not require a trellis. In contrast, coherent detection requires a trellis with Q states, where Q is the denominator of the modulation index $h = P/Q$ [1]. While h for the coherent detector must be rational, the noncoherent detector can work for any value of h. Furthermore, unlike the coherent detector, the noncoherent detector does not require knowledge of the initial phase or the set of allowable phases, which permits more robust operation.

If the channel- or oscillator-induced phase shift is stable over a block of several symbols, a *multisymbol* noncoherent detector can be used to exploit the phase continuity within each block [2]. In this paper, we evaluate multisymbol noncoherent detection from an information-theoretic perspective. In particular, we estimate the *average mutual information* (AMI) [3], which is the modulation-constrained channel capacity under the assumption of independent and uniformly distributed (i.u.d.) input symbols. We use AMI to determine the minimum required $\mathcal{E}_b/N_0$ under a bandwidth constraint, where $\mathcal{E}_b$ is the energy per information bit and N_0 is the one-sided noise-spectral density. For a particular modulation order, channel model, and receiver architecture, the minimum $\mathcal{E}_b/N_0$ is found by optimizing the AMI with respect to the modulation index h and code rate r. We show that the minimum required $\mathcal{E}_b/N_0$ decreases with increasing block size.

AMI has been previously used to characterize the achievable performance of several classes of coded modulation, though different authors use terms other than AMI. Caire et al. [3] use AMI to quantify the achievable capacity of quadrature amplitude modulation (QAM), phase shift keying (PSK), and orthogonal frequency-shift keying (FSK), though the authors use the term "coded modulation capacity" interchangeably with AMI. The achievable performance of *coherent* CPM is considered by Ganesan [4], who uses the term "independent and identically distributed (i.i.d.) capacity" instead of AMI, and by Padmanabham et al. [5], who simply use the term "capacity" even though only i.u.d. inputs are considered. In [6], AMI is called "symmetric information rate" (from [7]), and is used to jointly optimize the modulation index h and code rate r of coherent systems under a bandwidth constraint. In [8], the AMI of CPFSK was considered for single-symbol noncoherent reception and the modulation index and code rate were jointly optimized. By comparing the results for single-symbol noncoherent reception [8] against those for coherent reception [4]–[6], it can be concluded that the loss due to using single-symbol noncoherent reception is large. However, noncoherent reception is an attractive alternative to coherent receivers, which are typically more complex and impose a requirement for phase acquisition and tracking. The purpose of this paper is to bridge the gap between coherent and single-symbol noncoherent reception, which may be considered as limiting cases of the multisymbol noncoherent receiver with block lengths of either infinity or unity, respectively.

The issue of code design for CPM systems has also been considered in the literature. In [9], it is shown that placing

Paper approved by E. Perrins, the Editor for Modulation Theory of the IEEE Communications Society. Manuscript received August 6, 2009; revised December 3, 2009.

M. C. Valenti is with West Virginia University, Morgantown, WV (e-mail: valenti@ieee.org).

S. Cheng is with Applied Micro Circuits Corporation, Sunnyvale, CA (e-mail: shi.cheng@gmail.com).

D. Torrieri is with the US Army Research Laboratory, Adelphi, MD (e-mail: dtorr@arl.army.mil).

M. C. Valenti's contribution was sponsored by the National Science Foundation under Award No. CNS-0750821.

Portions of this paper were presented at the IEEE Military Communication Conference (MILCOM), Boston, MA, Oct. 2009.

Digital Object Identifier 10.1109/TCOMM.2010.07.090453

an interleaver between a convolutional code and a CPM modulator creates a type of serially-concatenated code, which is suitable for iterative reception using the soft-input, soft-output (SISO) algorithm [10]. In [11], the convolutional outer code of [9] is replaced with a set of irregular repeat codes. When coherently detected, the resulting structure is a type of irregular repeat accumulate (IRA) code and may be decoded over an appropriately defined factor graph. In [6], we optimize such a structure under a bandwidth constraint. In [12], we extend the IRA analogy to the multisymbol noncoherent receiver, but because the noncoherent receiver destroys the memory in the modulation, an error floor emerges. The error floor can be mitigated by differentially encoding the modulator input, though this comes at a cost of pushing the "turbo cliff" out to a higher $\mathcal{E}_b/N_0$.

The remainder of this paper is organized as follows. A model of CPFSK is given in Section II. The multisymbol noncoherent receiver is derived in Section III, and its complexity discussed in Section IV. The average mutual information of the system is discussed in Section V, and the system parameters are optimized in Section VI with respect to the average mutual information. In Section VII, simulation results are given showing the performance of multisymbol noncoherent detection when a standard turbo code is used.

II. System Model

Consider a *bit-interleaved coded modulation* (BICM) system [3]. The input to the system is a set of K data bits $\mathbf{b} = [b_1, ..., b_K]$, which are passed through a binary channel encoder to yield a length-N_c codeword $\mathbf{c} = [c_1, ..., c_{N_c}]$. The codeword is bitwise interleaved and mapped to a length-$N_q = N_c/\log_2 M$ vector $\mathbf{q} = [q_1, ..., q_{N_q}]$ of M-ary symbols, where each $q_i \in \{0, 1, ..., M-1\}$. The code rate is $r = K/N_q = K\log_2 M/N_c$ information bits per symbol.

For each entry of $\mathbf{q}$, the complex envelope of the continuous-time modulated signal $x_i(t)$ is chosen as the q_i^{th} signal of the set of continuous-time signals $\mathcal{S} = \{s_k(t), k = 0, 1, \cdots, M-1\}$, where

$$s_k(t) \quad = \quad \frac{1}{\sqrt{T_s}} e^{\frac{j2\pi kht}{T_s}}, \quad t \in [0, T_s), \tag{1}$$

h is the *modulation index*, T_s is the symbol duration, and $j = \sqrt{-1}$. In order to produce a more compact spectrum, an additional phase ϕ_i is applied so that the phase transition from symbol to symbol is continuous. This additional phase is accumulated as

$$\phi_{i+1} \quad = \quad 2\pi q_i h + \phi_i. \tag{2}$$

The transmitted signal is $\mathrm{Re}\left\{e^{j\phi_i} x_i(t) e^{j2\pi f_c t}\right\}$, where f_c is the frequency of the lowest tone and $\mathrm{Re}\{\cdot\}$ indicates the real part. The signal is transmitted over a block-fading channel. During the interval $iT_s \le t \le (i+1)T_s$, the complex envelope of the received signal is

$$y_i(t) \quad = \quad a_{\lfloor i/L \rfloor} e^{j\theta_{\lfloor i/L \rfloor}} e^{j\phi_i} \sqrt{\mathcal{E}_s} x_i(t) + n_i(t) \tag{3}$$

where $n_i(t)$ is additive white Gaussian noise (AWGN) with noise spectral density N_0, $\mathcal{E}_s$ is the energy per symbol, L is the channel block length, $a_k e^{j\theta_k}$ is the complex fading coefficient of channel block $k = \lfloor \frac{i}{L} \rfloor$, and the function $\lfloor x \rfloor$ rounds x down to an integer value. Two types of block channels are considered: Rayleigh-fading and AWGN channels that allow for an unknown phase when noncoherent detection is used. In both channels, θ_k is uniformly distributed over the range $[0, 2\pi)$ and independent from one block to the next. For the AWGN channel $a_k = 1, \forall k$. In the block Rayleigh fading channel, the a_k's are Rayleigh distributed with equal energy $E[a_k^2] = 1, \forall k$, and are independent from one block to the next. Block fading may be used to model a time-varying channel with coherence-time on the order of a block length.

The front-end of the detector is a bank of M pairs of matched filters, with one pair matched to the in-phase and quadrature components of each tone in $\mathcal{S}$. The matched filters are sampled at the symbol rate. At the end of the i^{th} symbol period, the outputs of the matched filters are placed into the $M \times 1$ complex vector

$$\mathbf{y}_i \quad = \quad a_{\lfloor i/L \rfloor} e^{j\psi_i} \sqrt{\mathcal{E}_s} \mathbf{x}_i + \mathbf{n}_i \tag{4}$$

where $\psi_i = \theta_{\lfloor i/L \rfloor} + \phi_i$ is the received phase at the start of the i^{th} symbol period, $\mathbf{x}_i$ is a signal vector, and $\mathbf{n}_i$ is a Gaussian-noise vector. Because the signals in $\mathcal{S}$ are not necessarily orthogonal, the noise $\mathbf{n}_i$ will generally be colored, and $\mathbf{x}_i$ will generally be represented by a complex, non-elementary vector. The properties of $\mathbf{x}_i$ and $\mathbf{n}_i$ are discussed next.

For ease of exposition, consider a single symbol and drop the subscript i. The signal vector is thus

$$\mathbf{y} \quad = \quad a e^{j\psi} \sqrt{\mathcal{E}_s} \mathbf{x} + \mathbf{n}. \tag{5}$$

The elements of $\mathbf{x}$ and $\mathbf{n}$ are found by correlating the signal $x(t)$ and noise $n(t)$ with each signal $s_k(t) \in \mathcal{S}, k = \{0, 1, ..., M-1\}$, giving

$$x_k \quad = \quad \int_0^{T_s} x(t) s_k^*(t) dt \tag{6}$$

$$n_k \quad = \quad \int_0^{T_s} n(t) s_k^*(t) dt \tag{7}$$

where $s_k^*(t)$ is the complex conjugate of $s_k(t)$.

Define the $M \times M$ matrix $\mathbf{K}$ whose $(\ell, m)^{th}$ element is the correlation of signal $s_m(t)$ with signal $s_\ell(t)$,

$$\begin{aligned} K_{\ell,m} &= \int_0^{T_s} s_m(t) s_\ell^*(t) dt \\ &= \frac{1}{T_s} \int_0^{T_s} \exp\left\{\frac{j2\pi(m-\ell)ht}{T_s}\right\} dt \\ &= \frac{\sin(\pi(m-\ell)h)}{\pi(m-\ell)h} e^{j\pi(m-\ell)h}. \end{aligned} \tag{8}$$

Note that the main diagonal of $\mathbf{K}$ is all ones. When h is an integer, the off-diagonal terms are zero, and the modulation is orthogonal. On the other hand, when h is not an integer, the off-diagonal terms are complex values representing the inter-tone correlation. Note also that when $x(t) = s_q(t)$, the signal vector $\mathbf{x} = \mathbf{k}_q$ where $\mathbf{k}_q$ represents the q^{th} column of $\mathbf{K}$. Thus, the columns of $\mathbf{K}$ comprise the signal set for the discrete-time model, i.e., the discrete-time $\mathcal{S} = \{\mathbf{k}_1, ...\mathbf{k}_{M-1}\}$.

The covariance of the noise is the $M \times M$ matrix $\mathbf{R} = \mathbf{E}(\mathbf{n}\mathbf{n}^H)$ with $(\ell, m)^{th}$ element

$$\begin{aligned} R_{\ell,m} &= E[\mathbf{n}_\ell \mathbf{n}_m^*] \\ &= E\left[\int_0^{T_s} n(\lambda) s_\ell^*(\lambda) d\lambda \int_0^{T_s} n^*(t) s_m(t) dt\right] \\ &= \int_0^{T_s} s_m(t) \underbrace{\int_0^{T_s} s_\ell^*(\lambda) \underbrace{E\left[n(\lambda) n^*(t)\right]}_{N_0 \delta(\lambda - t)} d\lambda}_{N_0 s_\ell^*(t)} dt \\ &= N_0 K_{\ell,m}. \end{aligned} \tag{9}$$

Since $\mathbf{n}$ is Gaussian, the vector $\mathbf{y}$ given the transmitted symbol q, amplitude $a\sqrt{\mathcal{E}_s}$, and phase ψ is Gaussian distributed with mean $\mathbf{m}_q = ae^{j\psi}\sqrt{\mathcal{E}_s}\mathbf{k}_q$ and covariance $\mathbf{R} = N_0\mathbf{K}$. The conditional joint probability density function (pdf), $p(\mathbf{y}|q, a\sqrt{\mathcal{E}_s}, \psi)$, has exponent

$$\begin{aligned} &-(\mathbf{y} - \mathbf{m}_q)^H \mathbf{R}^{-1} (\mathbf{y} - \mathbf{m}_q) \\ &\quad = 2\mathrm{Re}(\mathbf{m}_q^H \mathbf{R}^{-1} \mathbf{y}) - \mathbf{y}^H \mathbf{R}^{-1} \mathbf{y} - \mathbf{m}_q^H \mathbf{R}^{-1} \mathbf{m}_q \\ &\quad = 2\frac{a\sqrt{\mathcal{E}_s}}{N_0} \mathrm{Re}\left\{e^{-j\psi} y_q\right\} - \frac{\mathbf{y}^H \mathbf{K}^{-1} \mathbf{y} + a^2 \mathcal{E}_s}{N_0} \end{aligned} \tag{10}$$

where y_q is the q^{th} component of the vector $\mathbf{y}$, and the last line follows from the fact that $\mathbf{k}_q^H \mathbf{K}^{-1}$ is the row vector with "1" in position q and zeros elsewhere and $\mathbf{k}_q^H \mathbf{K}^{-1} \mathbf{k}_q = 1$. Using (10) as the exponent of the conditional pdf and discarding terms that are common to all hypotheses, the conditional likelihood for each postulated symbol q is

$$p(\mathbf{y}|q, a\sqrt{\mathcal{E}_s}, \psi) \quad \propto \quad \exp\left(2\frac{a\sqrt{\mathcal{E}_s}}{N_0} \mathrm{Re}\left\{e^{-j\psi} y_q\right\}\right) \tag{11}$$

where $\propto$ is read as "is proportional to".

III. Multisymbol Noncoherent Detection

When the channel block length L is sufficiently long, a multisymbol noncoherent detector of block length N may be used, provided that $N \leq L$. Let $\tilde{\mathbf{q}} = [q_0, ..., q_{N-1}]$ denote a block of N consecutive symbols and $\tilde{\mathbf{x}} = [\mathbf{x}_0, \cdots, \mathbf{x}_{N-1}]$ denote the corresponding block of N symbol vectors. Let $\tilde{\boldsymbol{\psi}} = [\psi_0, \cdots, \psi_{N-1}]$ be the set of N phase shifts corresponding to $\tilde{\mathbf{q}}$ with initial phase ϕ_0, where $\psi_i = \phi_i + \theta$ and θ is the channel phase for the block (assumed constant since $N \leq L$). Let $\tilde{\mathbf{y}} = [\mathbf{y}_0, \cdots, \mathbf{y}_{N-1}]$ be the received block of N signal vectors. The multisymbol noncoherent detector computes the probability $p(\tilde{\mathbf{y}}|\tilde{\mathbf{q}})$ for each of the M^N possible $\tilde{\mathbf{q}}$. By using the chain rule and the properties of Markov chains, the conditional probability of receiving block $\tilde{\mathbf{y}}$ given the postulated symbol block $\tilde{\mathbf{q}}$, the received amplitude $a\sqrt{\mathcal{E}_s}$, and the phases $\tilde{\boldsymbol{\psi}}$ is

$$p\left(\tilde{\mathbf{y}}|\tilde{\mathbf{q}}, a\sqrt{\mathcal{E}_s}, \tilde{\boldsymbol{\psi}}\right) \quad = \quad \prod_{i=0}^{N-1} p\left(\mathbf{y}_i|q_i, a\sqrt{\mathcal{E}_s}, \psi_i\right). \tag{12}$$

Substituting (11) into (12), the conditional likelihood given the postulated symbol block $\tilde{\mathbf{q}}$ is

$$p\left(\tilde{\mathbf{y}}|\tilde{\mathbf{q}}, a\sqrt{\mathcal{E}_s}, \tilde{\boldsymbol{\psi}}\right) \quad \propto \quad \exp\left(2\frac{a\sqrt{\mathcal{E}_s}}{N_0} \mathrm{Re}\left\{e^{-j\psi_0} \mu(\tilde{\mathbf{q}})\right\}\right) \tag{13}$$

where (2) implies that

$$\mu\left(\tilde{\mathbf{q}}\right) \quad = \quad \sum_{i=0}^{N-1} y_{q_i,i} \exp\left\{-j2h\pi \sum_{k=0}^{i-1} q_k\right\} \tag{14}$$

and $y_{q_i,i}$ is the q_i^{th} element of received vector $\mathbf{y}_i$. Using the fact that $\tilde{\boldsymbol{\psi}}$ is a function of $\{\tilde{\boldsymbol{q}}, \psi_0\}$ and marginalizing (13) with respect to ψ_0, which is assumed to be uniform over $[0, 2\pi)$, yields

$$p\left(\tilde{\mathbf{y}}|\tilde{\mathbf{q}}, a\sqrt{\mathcal{E}_s}\right) \quad \propto \quad I_0\left(2\frac{a\sqrt{\mathcal{E}_s}}{N_0} \left|\mu\left(\tilde{\mathbf{q}}\right)\right|\right) \tag{15}$$

where $I_0(\cdot)$ is the 0^{th} order modified Bessel function of the first kind.

The multisymbol detector works as follows. For each hypothesis $\tilde{\mathbf{q}}$ of the M^N hypotheses, it computes the conditional likelihood using (15) or its logarithm. A hard-decision detector merely takes the hypothesis that maximizes the likelihood. Alternatively, to enable soft-decision decoding of a binary code, the demodulator computes the log-likelihood ratio (LLR) for each code bit. For the k^{th} code bit in the block, the LLR is [13]

$$\lambda_k \quad = \quad \log \frac{\sum_{\tilde{\mathbf{q}}: b_k(\tilde{\mathbf{q}})=1} p\left(\tilde{\mathbf{y}}|\tilde{\mathbf{q}}, a\sqrt{\mathcal{E}_s}\right) P\left[\mathbf{b}(\tilde{\mathbf{q}}) \backslash b_k(\tilde{\mathbf{q}})\right]}{\sum_{\tilde{\mathbf{q}}: b_k(\tilde{\mathbf{q}})=0} p\left(\tilde{\mathbf{y}}|\tilde{\mathbf{q}}, a\sqrt{\mathcal{E}_s}\right) P\left[\mathbf{b}(\tilde{\mathbf{q}}) \backslash b_k(\tilde{\mathbf{q}})\right]} \tag{16}$$

where $\mathbf{b}\left(\tilde{\mathbf{q}}\right) = [b_0, ..., b_{\kappa-1}]$ is the set of $\kappa = N \log_2 M$ code bits associated with hypothetical block of symbols $\tilde{\mathbf{q}}$, the function $b_k(\tilde{\mathbf{q}})$ returns the k^{th} entry of the vector $\mathbf{b}(\tilde{\mathbf{q}})$, and $P[\mathbf{b}(\tilde{\mathbf{q}}) \backslash b_k(\tilde{\mathbf{q}})]$ is the *a priori* probability of $\mathbf{b}(\tilde{\mathbf{q}})$ excluding bit $b_k(\tilde{\mathbf{q}})$.

The LLR is most efficiently computed in the logarithmic domain. This is accomplished by defining $v_j = \log\left(P[b_j\left(\tilde{\mathbf{q}}\right) = 1] / P[b_j\left(\tilde{\mathbf{q}}\right) = 0]\right)$ to be the *a priori* LLR of bit j and using the max-star operator [14],

$$\max_{x \in \mathcal{X}} *(x) \quad = \quad \log \sum_{x \in \mathcal{X}} e^x. \tag{17}$$

Substituting (15) into (16) yields the log-domain expression

$$\begin{aligned} \lambda_k \quad = \quad & \max_{\tilde{\mathbf{q}}: b_k(\tilde{\mathbf{q}})=1} * \left[\log I_0\left(2\frac{a\sqrt{\mathcal{E}_s}}{N_0} \left|\mu(\tilde{\mathbf{q}})\right|\right) + \sum_{\substack{j=0 \\ j \neq k}}^{\kappa-1} b_j\left(\tilde{\mathbf{q}}\right) v_j\right] \\ & - \max_{\tilde{\mathbf{q}}: b_k(\tilde{\mathbf{q}})=0} * \left[\log I_0\left(2\frac{a\sqrt{\mathcal{E}_s}}{N_0} \left|\mu(\tilde{\mathbf{q}})\right|\right) + \sum_{\substack{j=0 \\ j \neq k}}^{\kappa-1} b_j\left(\tilde{\mathbf{q}}\right) v_j\right]. \end{aligned} \tag{18}$$

In a non-iterative BICM receiver, the *a priori* probabilities are all equal and therefore may be dropped from the logarithm by setting all v_j in (18) to zero. In an iterative BICM receiver with soft feedback (cf. BICM with Iterative Decoding, or *BICM-ID* [13]), the *extrinsic* information fed back from the decoder may be used as an estimate for the *a priori* LLRs v_j. When $M = 2$ and $N = 1$, there is just a single bit per block, i.e. $\kappa = 1$, which eliminates the two summations in (18) and implies that there there is no benefit to iterating. However, when $M^N > 2$, there will be more than one bit per block and it becomes advantageous to iterate.

IV. Computational Complexity

The computational effort associated with the multisymbol noncoherent receiver may be determined by carefully inspecting equation (14) and (18). Equation (14) must be computed for each of the M^N hypothesis. The outer summation in (14) is over N complex terms, and therefore requires $2(N-1)$ real additions. Each term in (14) requires the complex multiplication of y_{q_i} with a factor $\exp\{-j2h\pi \sum q_k\}$ that may be stored in a table since it is a not a function of the received signal. Since a complex multiplication may be implemented with four real multiplications and two real additions, computing (14) for all of the hypothesis requires a total of $4NM^N$ real multiplications and $(4N-2)M^N$ real additions. As shown in (18), the magnitude of each of the $\mu(\tilde{\mathbf{q}})$ must be multiplied by a scaling factor $2a\sqrt{\mathcal{E}_s}/N_0$ and passed through the nonlinear function $\log I_0(\cdot)$, which may be implemented by a piecewise linear approximation [15]. In an iterative receiver, the $\log I_0(\cdot)$ terms may be stored in a table, since they do not depend on the extrinsic input returned from the decoder. The total per-block computational effort for computing the $\log I_0(\cdot)$ terms is equal to the sum of the effort for computing (14), taking the absolute value, multiplying by $2a\sqrt{\mathcal{E}_s}/N_0$, and passing through the $\log I_0(\cdot)$ function, which is a total of $(4N-2)M^N$ real additions, $(4N+1)M^N$ real multiplications, and M^N evaluations each of the absolute value and $\log I_0(\cdot)$ operators. These values constitute the overhead prior to doing any iterations.

For each receiver iteration, (18) is computed for each bit. Each of the two max-star operations in (18) is over $2^{\kappa-1}$ arguments and requires $2^{\kappa-1}-1$ pairwise max-star operations. Thus, the total number of pairwise max-star operations per bit and per iteration is $2^\kappa - 2$. The total number of additions per bit required by (18) is $(\kappa+1)2^{\kappa-2}$, which is equal to the total number of additions required by the arguments of the max-star operators and another addition to subtract the results of the two max-star operations. For each $\tilde{\mathbf{q}}$ whose binary expansion (excluding bit k) $\mathbf{b}(\tilde{\mathbf{q}})\backslash b_k$ has a Hamming weight of w, there will be w additions required by the first max-star operator (the summation requires $w-1$ additions and that result is added to the $\log I_0(\cdot)$ term). Since the total weight of sequences of length n is $n2^{n-1}$, the arguments to the first max-star operator require $(\kappa-1)2^{\kappa-2}$ additions. For every $\mathbf{b}(\tilde{\mathbf{q}})\backslash b_k$ used by the first max-star operator, there will be an identical one used by the second max-star operator, which can be stored. Thus, the second max-star operator only requires $2^{\kappa-1}-1$ additions, i.e. one for every nonzero $\mathbf{b}(\tilde{\mathbf{q}})\backslash b_k$.

It is informative to compare the computation effort of the multisymbol noncoherent receiver against that of a coherent receiver. The coherent receiver is implemented by using a trellis with Q states. As with the noncoherent receiver, there is some overhead in determining metrics prior to iterating. The metric for each branch is found by derotating the symbol by the phase associated with the particular state transition, and then multiplying by a scaling factor. See, for instance, equation (11) in [6]. Comparing the pre-iteration overhead of the coherent and noncoherent receiver is difficult because, on the one hand, the noncoherent receiver requires a nonlinear $\log I_0(\cdot)$ function that is not needed by the coherent receiver, but on the other hand, the coherent receiver needs to estimate the channel phase θ, which is not required by the noncoherent receiver. A fair comparison must account for the effort to estimate the phase θ, which can be difficult in fast fading situations and frequency-hopping applications.

Once the metrics have been determined, the coherent receiver performs log-MAP decoding, which requires a forward and reverse sweep through the trellis [14]. Each sweep requires $M-1$ pairwise max-star operations at each node in the trellis to obtain the corresponding state-transition likelihood. Since the total number of nodes in the length-N_q trellis is QN_q, the total number of pairwise max-star operations required to obtain the transition likelihoods is $2(M-1)QN_q$, or $2(M-1)Q/\log_2 M$ per bit. Once the transition likelihoods are obtained, finding each bit-likelihood requires a max-star operation over the $QM/2$ branches for which the bit is a one and the $QM/2$ branches for which the bit is a zero, and thus a total of $QM-2$ pairwise max-star operations are needed. Thus, the total number of max-star operations is $2(M-1)Q/\log_2 M + QM - 2$ per bit.

Having established the number of required max-star operations, it is now possible to compare the per-iteration complexity of the noncoherent and coherent receiver. Consider the case that $h = 3/5$ and therefore $Q = 5$, which is shown to be a good choice in Section VI. The coherent receiver requires 18 max-star operations per bit for binary ($M = 2$) CPFSK and 33 max-star operations per bit for quaternary ($M = 4$) CPFSK. If a block length of $N = 4$ is used, the noncoherent receiver requires 14 max-star operations per bit for the binary case, and 254 max-star operations per bit for the quaternary case.

V. Average Mutual Information

Consider the discrete-input, continuous-output channel with input block $\tilde{\mathbf{q}}$ and output block $\tilde{\mathbf{y}}$. The mutual information between the channel input and output is [16]

$$I(\tilde{\mathbf{q}};\tilde{\mathbf{y}}) = E\left[\log \frac{p(\tilde{\mathbf{y}}|\tilde{\mathbf{q}})}{p(\tilde{\mathbf{y}})}\right] \tag{19}$$

where $p(\tilde{\mathbf{y}})$ is the marginal pdf of $\tilde{\mathbf{y}}$, and $p\left(\tilde{\mathbf{y}}\middle|\tilde{\mathbf{q}}\right)$ is the conditional pdf of $\tilde{\mathbf{y}}$ given $\tilde{\mathbf{q}}$. When a base-2 logarithm is used, then (19) has units of bits per block.

The capacity of the channel is found by maximizing (19) with respect to the input distribution $p(\tilde{\mathbf{q}})$,

$$C = \max_{p(\tilde{\mathbf{q}})} I(\tilde{\mathbf{q}};\tilde{\mathbf{y}}). \tag{20}$$

When the optimization is carried out, the resulting discrete-input $\tilde{\mathbf{q}}$ might have a nonuniform distribution. Because most

practical systems assume that the inputs are constrained to be i.u.d., we assume that $p(\tilde{\mathbf{q}}) = M^{-N}$ for all possible $\tilde{\mathbf{q}}$. We follow the convention of Caire et al. [3] and refer to (19) with i.u.d. inputs as the *AMI*. We note that a nonuniform distribution may yield a slightly higher value for the mutual information, but finding the optimizing distribution and a practical coding scheme capable of inducing such a distribution are both nontrivial tasks that are outside the scope of this paper.

Let $\mathcal{Q}$ be the set of M^N possible values of $\tilde{\mathbf{q}}$. When the inputs are equally likely, $p(\tilde{\mathbf{y}}) = \sum_{\mathbf{q}' \in \mathcal{Q}} p(\tilde{\mathbf{y}}|\mathbf{q}')p(\mathbf{q}') = M^{-N} \sum_{\mathbf{q}' \in \mathcal{Q}} p(\tilde{\mathbf{y}}|\mathbf{q}')$, and we may rewrite (19) as

$$I(\tilde{\mathbf{q}};\tilde{\mathbf{y}}) \quad = \quad N \log M + E\left[\log \frac{p(\tilde{\mathbf{y}}|\tilde{\mathbf{q}})}{\sum_{\mathbf{q}' \in \mathcal{Q}} p(\tilde{\mathbf{y}}|\mathbf{q}')}\right]. \quad (21)$$

Substituting the conditional pdf of the multisymbol noncoherent detector given by (15) into (21) results in the AMI

$$I(\tilde{\mathbf{q}};\tilde{\mathbf{y}}) \quad = \quad N \log M + E\left[\log \frac{I_0\left(\frac{2a\sqrt{\mathcal{E}_s}|\mu(\tilde{\mathbf{q}})|}{N_0}\right)}{\sum\limits_{\mathbf{q}' \in \mathcal{Q}} I_0\left(\frac{2a\sqrt{\mathcal{E}_s}|\mu(\mathbf{q}')|}{N_0}\right)}\right] \quad (22)$$

where the expectation is taken over the ensemble of all possible transmitted $\tilde{\mathbf{q}}$ and received $\tilde{\mathbf{y}}$. To express (22) in terms of bits per channel use, use a base-2 logarithm and divide the result by N, i.e. the number of symbols per block.

Since it is an expectation, (22) may be computed using Monte Carlo simulation. To do this, first define a random variable

$$Z \quad = \quad \log I_0\left(\frac{2a\sqrt{\mathcal{E}_s}\,|\mu(\tilde{\mathbf{q}})|}{N_0}\right) - \log \sum_{\mathbf{q}' \in \mathcal{Q}} I_0\left(\frac{2a\sqrt{\mathcal{E}_s}\,|\mu(\mathbf{q}')|}{N_0}\right). \quad (23)$$

One realization of this random variable may be generated by picking a random $\tilde{\mathbf{q}}$, modulating it, passing it through a simulated channel to generate the corresponding $\tilde{\mathbf{y}}$, and then substituting the $\tilde{\mathbf{q}}$ and $\tilde{\mathbf{y}}$ into (23) with $\mu(\tilde{\mathbf{q}})$ as defined in (14). A large number of random variables can be generated this way and their average taken as an estimate of $E[Z]$. Finally, the average may be used to estimate the AMI $I(\tilde{\mathbf{q}};\tilde{\mathbf{y}}) = N \log M + E[Z]$.

As an example, Fig. 1 shows the AMI (in bits per channel symbol) of multisymbol noncoherent detection of minimum-shift keying (MSK), i.e. $h = 0.5$ and $M = 2$, for several different block sizes in AWGN. The rightmost curve ($N = 1$) is the AMI of single-symbol noncoherent detection [8], while the leftmost curve is the AMI with coherent reception [6]. By increasing N from 1 to 4, the gain at code-rate 0.5 is about 5 dB, and it is only 3.4 dB worse than coherent detection. As N increases, the AMI continues to approach that of coherent detection. As $N \to \infty$, we conjecture that the performance of multisymbol noncoherent reception converges to that of coherent reception since the two receivers become identical (except for knowledge of the initial phase ψ_0, which becomes irrelevant for sufficiently large N).

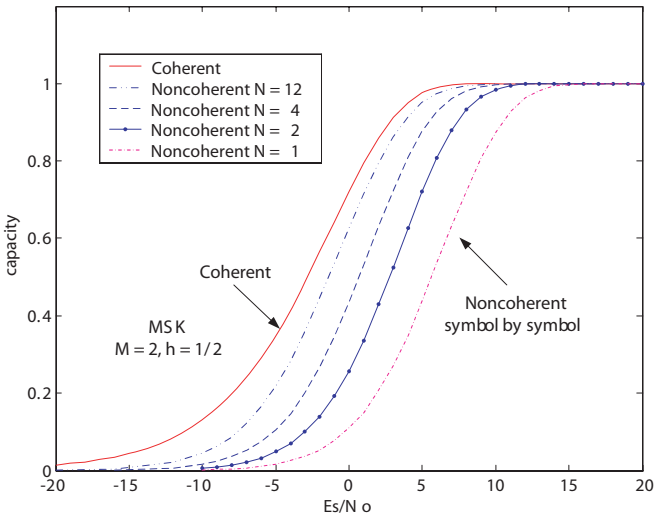

Fig. 1. Average mutual information of MSK over an AWGN channel with either N-symbol noncoherent detection or coherent detection.

VI. Bandwidth-Constrained Parameter Optimization

The bandwidth of coded CPFSK is a function of the modulation index, code rate, and modulation order. When the bandwidth is constrained to not exceed B_{max}, there is a particular combination of these parameters that minimizes the value of $\mathcal{E}_b/N_0$ required to achieve an arbitrarily low bit error rate. While one could search for the optimal combination of parameters by exhaustively simulating every possible choice of parameters with an actual capacity-approaching code, a more efficient way to search would be to leverage the information-theoretic analysis discussed in the previous section. The benefit of using AMI as a performance metric is that it provides a fairly accurate prediction of the performance that can be achieved with a capacity-approaching code without requiring that the code actually be simulated. Of course, once a good design is identified, it should be simulated using the proposed receiver and an actual code such as a turbo code, thereby confirming the effectiveness of the design.

In order to optimize under a bandwidth constraint, the influence of the system parameters upon bandwidth must be quantified. First consider an uncoded complex baseband signal $s(t)$ with power spectral density (PSD) $\Phi_s(f)$. Given the PSD, the 99% *power bandwidth* of the uncoded $s(t)$ is defined as the value of B_{99} that satisfies

$$\int_{-B_{99}/2}^{B_{99}/2} \Phi_s(f)df \quad = \quad 0.99 \int_{-\infty}^{\infty} \Phi_s(f)df. \quad (24)$$

The PSD $\Phi_s(f)$ of CPFSK is well known and can be found in texts such as Section 3.4-5 of [16]. When channel coding is used, the required bandwidth increases as the code rate decreases. Define the *normalized bandwidth* of the coded signal to be

$$\beta \quad = \quad \frac{B_{99}}{R_b} \quad (25)$$

where $R_b = r/T_s$ is the data rate in bits per second and β is in units of Hz/bps.

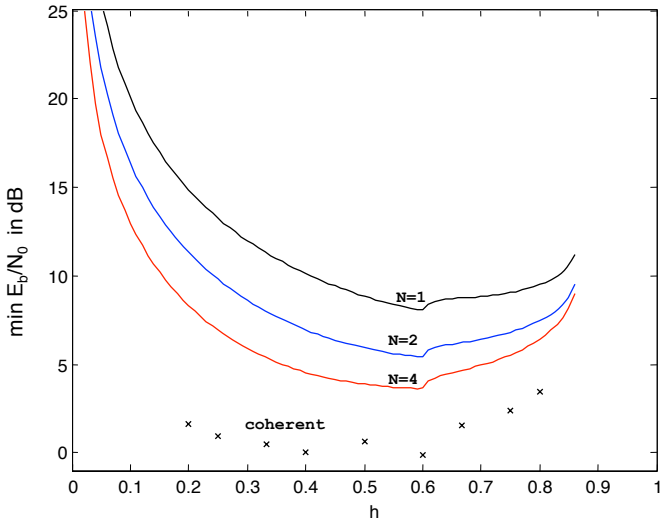

Fig. 2. Minimum $\mathcal{E}_b/N_0$ required for binary CPFSK to achieve an arbitrarily low error rate versus modulation index h in AWGN with $M = 2$ under bandwidth constraint $\beta_{max} = 2$ Hz/bps using N-symbol noncoherent detection with $N = \{1, 2, 4\}$. As a point of comparison, the minimum $\mathcal{E}_b/N_0$ required for coherent CPFSK is also shown [6].

Assume that the normalized bandwidth must not exceed a value β_{max}. The goal of the AMI-based optimization is to minimize the $\mathcal{E}_b/N_0$ required for reliable communication under this bandwidth constraint, which is achieved by jointly optimizing the parameters h and r for the given value of M, channel type (AWGN or fading), and decoder type (e.g., the block length N used by the multisymbol decoder). To perform the optimization, start with an arbitrary value of h. For this value of h, there will be a minimum permissible code rate r_{min}. Using a code rate lower than r_{min} with this h will violate the bandwidth constraint. For this h, the AMI $I(\tilde{\mathbf{q}}; \tilde{\mathbf{y}})$ is computed from (22) and plotted as a function of $\mathcal{E}_s/N_0$ (as was done in Fig. 1 for $h = 0.5$). Since $r \leq I(\tilde{\mathbf{q}}; \tilde{\mathbf{y}})$ is required for error-free decoding [3], $I(\tilde{\mathbf{q}}; \tilde{\mathbf{y}})$ monotonically increases with $\mathcal{E}_s/N_0$, and $r \geq r_{min}$ is required to satisfy the bandwidth requirement, it follows that the minimum $\mathcal{E}_s/N_0$ is the value for which $I(\tilde{\mathbf{q}}; \tilde{\mathbf{y}}) = r_{min}$. Next, the corresponding $\mathcal{E}_b/N_o = (\mathcal{E}_s/N_o)/r_{min}$ is determined. This will normally be the minimum $\mathcal{E}_b/N_o$ required for this value of h. However, due to the noncoherent-combining penalty, it is possible that a rate higher than r_{min} will provide a lower required $\mathcal{E}_b/N_o$ despite having a normalized bandwidth that is actually less than β_{max}. Thus, in order to account for this possibility, all rates $r \in [r_{min}, \log_2 M]$ must be considered when searching for the minimum $\mathcal{E}_b/N_o$.

The above procedure will give the minimum $\mathcal{E}_b/N_o$ and the optimum code rate for each valid value of h that is considered. In order to determine the global minimum, the process must be repeated for all h. In practice, it is sufficient to consider closely sampled values of h. Note that there is an upper limit on h such that even if a full-rate code were used (i.e. $r = \log_2 M$), the bandwidth constraint would be violated.

Optimizations were performed to determine the minimum $\mathcal{E}_b/N_0$ under a bandwidth constraint of $\beta_{max} = 2$ Hz/bps with $M = \{2, 4\}$ and $N = \{1, 2, 4\}$ over both AWGN and Rayleigh fading channels. The results of the optimization are shown in Figs. 2 through 5 and summarized in Table I. In the simulations used to compute the AMI, the channel block length is set to $L = N$. While a larger value of L could have been selected, the AMI does not depend on the value of L provided that $L \geq N$ and a sufficiently large number of trials is performed. For each value of N, the minimum $\mathcal{E}_b/N_0$ was determined for values of h that are multiples of 0.01. As a point of comparison, the minimum $\mathcal{E}_b/N_0$ for coherent CPFSK is shown for specific values of h, namely those $h = P/Q$ with integer Q satisfying $2 \leq Q \leq 5$. The values for coherent reception are from [6] for the AWGN channel[1].

TABLE I
MINIMUM REQUIRED $\mathcal{E}_b/N_0$ FOR $\beta_{max} = 2$ HZ/BPS.

		AWGN			Rayleigh Fading		
M	N	$\mathcal{E}_b/N_0$	h	r	$\mathcal{E}_b/N_0$	h	r
2	1	8.08 dB	0.60	0.64	10.69 dB	0.59	0.63
	2	5.43 dB	0.60	0.64	7.96 dB	0.56	0.61
	4	3.63 dB	0.59	0.63	6.12 dB	0.56	0.61
4	1	5.33 dB	0.67	0.78	8.17 dB	0.45	0.58
	2	3.51 dB	0.55	0.69	5.87 dB	0.43	0.57
	4	2.20 dB	0.48	0.61	4.31 dB	0.40	0.54

Fig. 2 shows results for the AWGN channel with $M = 2$ tones. For each type of receiver, the required $\mathcal{E}_b/N_0$ is minimized at or about $h = 0.6$. The corresponding code rate for this value of h is $r = 0.64$ (the bandwidth constraint is too tight for the noncoherent-combining penalty to require an r greater than this minimum). For conventional single-symbol noncoherent detection ($N = 1$), the system requires $\mathcal{E}_b/N_0 = 8.08$ dB, while for coherent detection the system requires $\mathcal{E}_b/N_0 = -0.10$ dB. This gap is bridged by multisymbol noncoherent reception, as is evident by inspecting Table I. Using length $N = 4$ blocks will provide a gain of over 4.4 dB relative to single-symbol noncoherent detection in an AWGN channel. However, for $M = 2$, there is still a loss of about 3.7 dB when using 4-block multisymbol noncoherent detection instead of coherent detection.

Fig. 3 shows results for the Rayleigh fading channel with $M = 2$. For this bandwidth constraint, the value of h that minimizes the required $\mathcal{E}_b/N_0$ with multisymbol noncoherent reception is slightly below $h = 0.6$. Similar to the AWGN channel, there is a gain of more than 4.5 dB when length $N = 4$ blocks are used instead of conventional single-symbol detection.

The results for quaternary CPFSK ($M = 4$) are shown in Fig. 4 for the AWGN channel and Fig. 5 for the Rayleigh fading channel. With coherent reception, the minimum $\mathcal{E}_b/N_0$ in AWGN for $M = 4$ is -0.32 dB. The gain of $N = 4$ multisymbol noncoherent reception in AWGN is about 3.1 dB relative to single-symbol noncoherent reception, though $N = 4$ multisymbol noncoherent reception has a loss of 2.5 dB relative to coherent reception. The gain achieved by increasing M from 2 to 4 is only 0.22 dB for the coherent receiver, but for the noncoherent receiver it is 2.75 dB, 1.92 dB, and 1.43 dB for $N = 1, 2$, and 4, respectively. This suggests

[1]The results for coherent CPFSK in Rayleigh fading were obtained as follows. Let $I(\tilde{\mathbf{q}}; \tilde{\mathbf{y}}|\gamma)$ be the AMI of an AWGN channel with SNR γ and coherent reception, which is found using the techniques in [6]. The AMI $I(\tilde{\mathbf{q}}; \tilde{\mathbf{y}})$ in Rayleigh fading is found by taking the expectation of $I(\tilde{\mathbf{q}}; \tilde{\mathbf{y}}|\gamma)$, i.e. $I(\tilde{\mathbf{q}}; \tilde{\mathbf{y}}) = E[I(\tilde{\mathbf{q}}; \tilde{\mathbf{y}}|\gamma)]$, where the expectation is with respect to the exponentially-distributed γ.

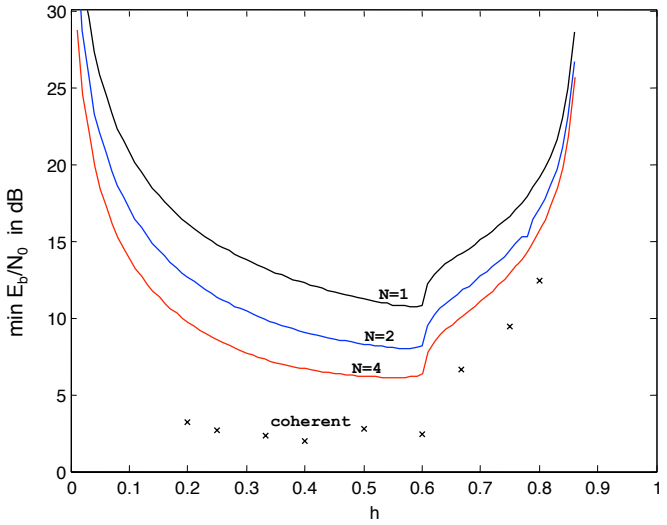

Fig. 3. Minimum $\mathcal{E}_b/N_0$ required for binary CPFSK to achieve an arbitrarily low error rate versus modulation index h in Rayleigh fading with $M = 2$ under bandwidth constraint $\beta_{max} = 2$ Hz/bps using N-symbol noncoherent detection with $N = \{1, 2, 4\}$. As a point of comparison, the minimum $\mathcal{E}_b/N_0$ required for coherent CPFSK is also shown.

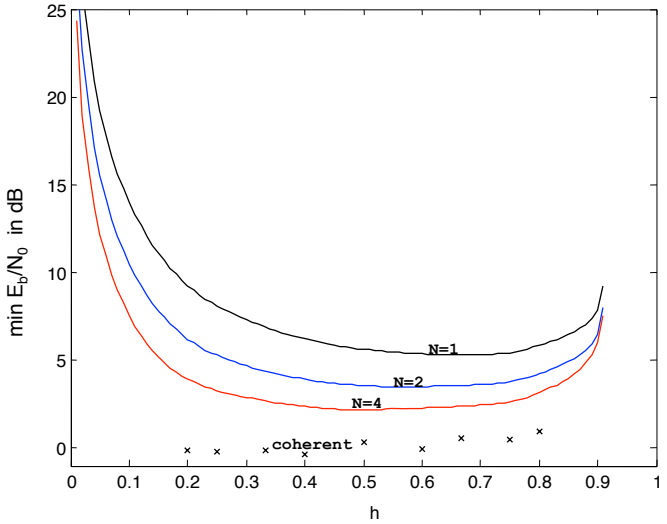

Fig. 4. Minimum $\mathcal{E}_b/N_0$ required for binary CPFSK to achieve an arbitrarily low error rate versus modulation index h in AWGN with $M = 4$ under bandwidth constraint $\beta_{max} = 2$ Hz/bps using N-symbol noncoherent detection with $N = \{1, 2, 4\}$. As a point of comparison, the minimum $\mathcal{E}_b/N_0$ required for coherent CPFSK is also shown [6].

that the multisymbol noncoherent receiver is better able to exploit the larger signal set than does the coherent receiver. The gain of $N = 4$ multisymbol noncoherent reception in the Rayleigh fading channel with $M = 4$ is 3.86 dB relative to single-symbol noncoherent reception. For the multisymbol noncoherent receiver, the gain from using $M = 4$ instead of $M = 2$ is 2.52 dB, 2.09 dB, and 1.81 dB for $N = 1, 2$, and 4, respectively, again demonstrating that the multisymbol noncoherent receiver is able to exploit the larger signal set.

VII. Turbo-Coded Performance

Simulations were performed to demonstrate the achievable performance when an actual channel code is used, thereby confirming the relevance of the information-theoretic bounds.

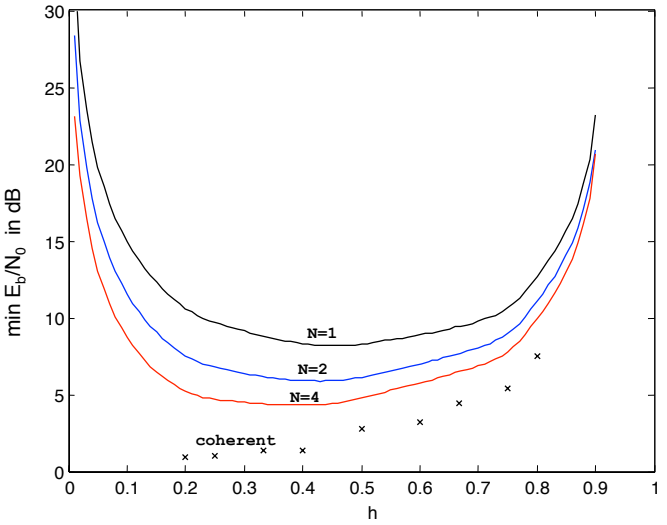

Fig. 5. Minimum $\mathcal{E}_b/N_0$ required for binary CPFSK to achieve an arbitrarily low error rate versus modulation index h in Rayleigh fading with $M = 4$ under bandwidth constraint $\beta_{max} = 2$ Hz/bps using N-symbol noncoherent detection with $N = \{1, 2, 4\}$. As a point of comparison, the minimum $\mathcal{E}_b/N_0$ required for coherent CPFSK is also shown.

Systems with CPFSK modulation and $M = 2$ and $M = 4$ were considered. For systems with $M = 2$, the modulation index was set to $h = 0.6$, which is the optimal value for the single-symbol noncoherent detector under bandwidth constraint $\beta_{max} = 2$ Hz/bps according to the information-theoretic analysis given in the last section. The code rate was set to its corresponding optimal value $r = 0.64$. Data was encoded using the turbo code specified by the UMTS standard [17], which was selected due to its widespread use and its ability to handle a variety of code rates. The rate $r = 0.64$ was achieved by using a message length of $K = 4800$ bits and a codeword length of $N_c = 7500$ bits. The demodulator was implemented using the proposed noncoherent N-symbol demodulator with $N = 1, 2$, and 4. The turbo code was decoded using 30 iterations of the log-MAP algorithm [16]. When $M^N > 2$, a BICM-ID receiver was used, in which case the soft-output from each decoder iteration was used by the demodulator as *a priori* information.

Simulations were run for both an AWGN channel and a Rayleigh fading channel. Fig. 6 shows results for the AWGN channel with $M = 2$. Three curves are shown corresponding to length $N = 1, 2$, and 4 demodulator blocks. In addition, a vertical line is shown for each value of N that corresponds to the minimum $\mathcal{E}_b/N_0$ found from the previous information-theoretic analysis. The value of $\mathcal{E}_b/N_0$ required for the turbo-coded system to achieve a BER of 10^{-5} in AWGN is 8.90 dB, 6.13 dB, and 4.44 dB for $N = 1, 2$, and 4, respectively. These values are between 0.80 and 0.98 dB from the corresponding information-theoretic bounds, indicating that it is possible to design a system that performs within a decibel of the bounds.

Fig. 7 shows results for the Rayleigh fading channel with $M = 2$. In the simulations, the fading amplitude was held constant for blocks of L consecutive symbols and varied independently from one block to the next. In order to maximize the number of independent fades per codeword, we set L equal to N, which is the minimum value required by the

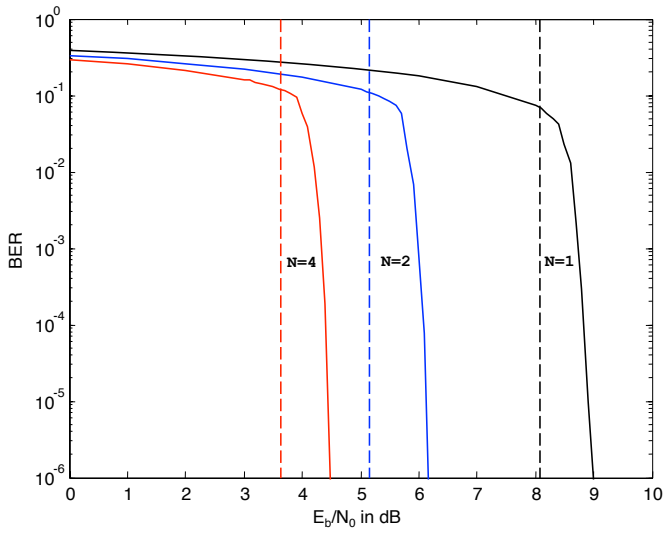

Fig. 6. BER vs. $\mathcal{E}_b/N_0$ in AWGN of a CPFSK system using $M = 2, h = 0.6, r = 0.64$ and N-symbol noncoherent detection with $N = \{1, 2, 4\}$.

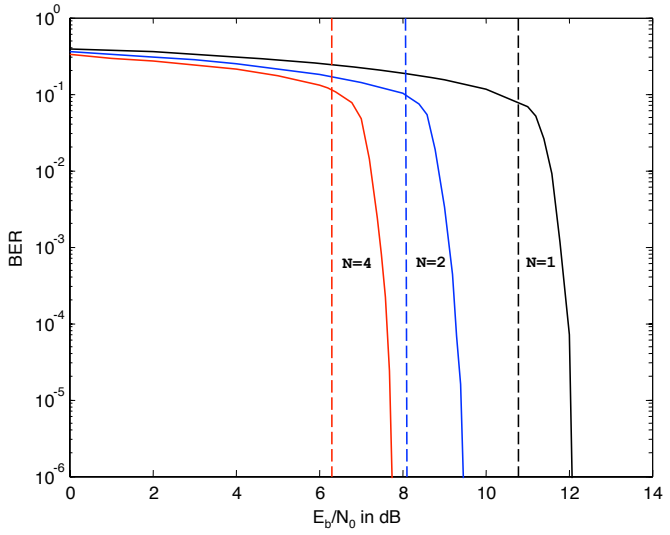

Fig. 7. BER vs. $\mathcal{E}_b/N_0$ in Rayleigh fading of a CPFSK system using $M = 2, h = 0.6, r = 0.64$ and N-symbol noncoherent detection.

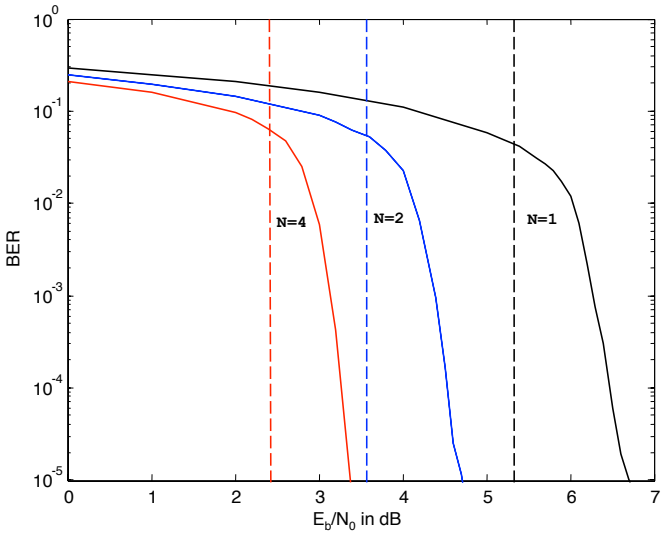

Fig. 8. BER vs. $\mathcal{E}_b/N_0$ in AWGN of a CPFSK system using $M = 4, h = 0.67, r = 0.78$ and N-symbol noncoherent detection with $N = \{1, 2, 4\}$.

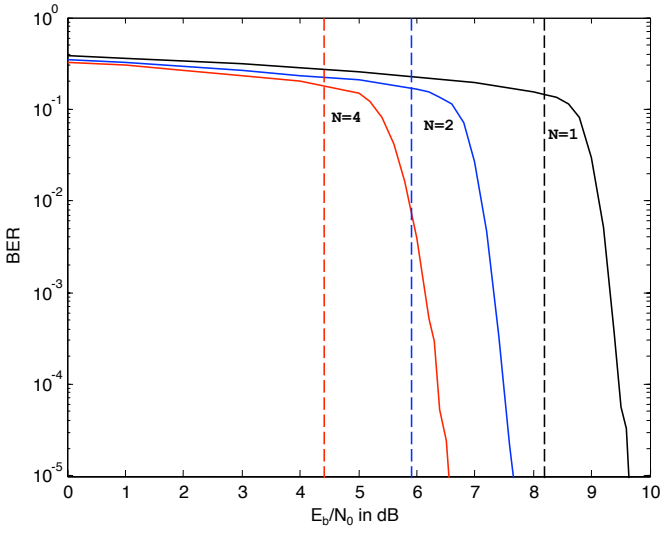

Fig. 9. BER vs. $\mathcal{E}_b/N_0$ in Rayleigh fading of a CPFSK system using $M = 4, h = 0.45, r = 0.58$ and N-symbol noncoherent detection.

multisymbol noncoherent detector. As in the previous figure, a vertical line is shown for each value of N that corresponds to the minimum $\mathcal{E}_b/N_0$ found from the information-theoretic analysis. The value of $\mathcal{E}_b/N_0$ required for the turbo-coded system to achieve a BER of 10^{-5} in Rayleigh fading is 12.04 dB, 9.41 dB, and 7.72 dB for $N = 1, 2$, and 4, respectively. These values are between 1.26 and 1.41 dB from the corresponding information-theoretic bounds. While the gap between the theoretical $\mathcal{E}_b/N_0$ and the value required with the actual turbo code is slightly higher for Rayleigh fading than it is for AWGN, it is feasible to design a system that can come within 1.5 dB of the bounds in Rayleigh fading.

For systems with $M = 4$, the modulation index was set to $h = 0.67$ for the AWGN channel and $h = 0.45$ for the Rayleigh fading channel. These are the information-theoretic optimal values for the single-symbol noncoherent detector under bandwidth constraint $\beta_{max} = 2$ Hz/bps. The UMTS standard turbo code was again used, with the rate set to $r = 5100/6528$ for the AWGN channel and $r = 3800/6528$ for the Rayleigh fading channel. The codeword length was 6528 bits for both channels. For all values of N, 30 iterations of BICM-ID reception were performed by using a combination of the proposed receiver and the log-MAP decoding algorithm.

Fig. 8 shows results for the AWGN channel with $M = 4$ and three values of N. The value of $\mathcal{E}_b/N_0$ required for the turbo-coded system to achieve a BER of 10^{-5} in AWGN is 6.70 dB, 4.72 dB, and 3.37 dB for $N = 1, 2$, and 4, respectively. These values are between 0.94 and 1.37 dB from the corresponding information-theoretic bounds, which are indicated by the dashed lines.

Fig. 9 shows results for the Rayleigh fading channel with $M = 4$. The value of $\mathcal{E}_b/N_0$ required for the turbo-coded system to achieve a BER of 10^{-5} in Rayleigh fading is 9.63 dB, 7.65 dB, and 6.54 dB for $N = 1, 2$, and 4, respectively. These values are between 1.44 and 2.13 dB from the corresponding information-theoretic bounds.

VIII. Conclusion

Multisymbol noncoherent demodulation is an attractive compromise between coherent demodulation, which requires the additional complexity of requiring the phase to be estimated and tracked, and single-symbol noncoherent demodulation, which has poor energy efficiency. The performance of a multisymbol noncoherent system can be improved by using a capacity-approaching code, such as a turbo code. To fully exploit the benefits of the channel code, the demodulator developed in this paper uses soft-input, soft-output demodulation over blocks of multiple received symbols.

The performance of a system that uses a capacity-approaching code and the proposed demodulator may be predicted by using the average mutual information. The performance depends on several parameters, including the choice of modulation index h and code rate r. When there is a bandwidth constraint, there is a combination of h and r that minimizes the $\mathcal{E}_b/N_0$ required for reliable signaling. The average mutual information can be used to identify the optimal values of these parameters for a particular bandwidth constraint, modulation order M, demodulator block length N, and channel type. When the optimal parameters are chosen and binary modulation is used, the 4-symbol demodulator outperforms the single-symbol demodulator by about 4.4-4.5 dB in both AWGN and Rayleigh fading channels, yet is still about 3.7 dB worse than the coherent demodulator.

Once the optimal parameters have been identified, a complete system can be designed by incorporating an outer error-correcting code. While the code could be optimized for the particular system, reasonable performance can be achieved by using an "off-the-shelf" standardized code. In particular, if the standardized UMTS turbo-code is used with $M = 2$ tones, then performance within 1 dB of the information-theoretic bound can be achieved in AWGN and performance within 1.5 dB of the bound can be achieved over a Rayleigh fading channel. When $M = 4$ tones are used with the UMTS turbo code, performance is within 1.4 dB of the information-theoretic bound in AWGN and within 2.2 dB of the bound in Rayleigh fading.

References

[1] B. Rimoldi, "A decomposition approach to CPM," *IEEE Trans. Inf. Theory*, vol. 34, pp. 260-270, Mar. 1988.

[2] M. K. Simon and D. Divsalar, "Maximum-likelihood block detection of noncoherent continuous phase modulation," *IEEE Trans. Commun.*, vol. 41, pp. 90-98, Jan. 1993.

[3] G. Caire, G. Taricco, and E. Biglieri, "Bit-interleaved coded modulation," *IEEE Trans. Inf. Theory*, vol. 44, pp. 927-946, May 1998.

[4] A. Ganesan, "Capacity estimation and code design principles for continuous phase modulation (CPM)," master's thesis, Texas A&M University, College Station, TX, May 2003.

[5] K. Padmanabhan, S. Ranganathan, S. P. Sundaravaradham, and O. M. Collins, "General CPM and its capacity," in *Proc. IEEE Int. Symp. Inf. Theory (ISIT)*, Adelaide, Australia, pp. 750-754, Sep. 2005.

[6] S. Cheng, M. C. Valenti, and D. Torrieri, "Coherent continuous-phase frequency-shift keying: parameter optimization and code design," *IEEE Trans. Wireless Commun.*, vol. 8, pp. 1792-1802, Apr. 2009.

[7] H. Pfister, J. Soriaga, and P. Siegel, "On the achievable information rates of finite state ISI channels," in *Proc. IEEE Global Telecommun. Conf. (GLOBECOM)*, San Anotonio, TX, Nov. 2001.

[8] S. Cheng, R. I. Seshadri, M. Valenti, and D. Torrieri, "The capacity of noncoherent continuous-phase frequency shift keying," in *Proc. Conf. Inf. Sciences Syst. (CISS)*, Baltimore, MD, Mar. 2007.

[9] K. R. Narayanan and G. L. Stüber, "Performance of trellis-coded CPM with iterative demodulation and decoding," *IEEE Trans. Commun.*, vol. 49, pp. 676-687, Apr. 2001.

[10] S. Benedetto, D. Divsalar, G. Montorsi, and F. Pollara, "A soft-input soft-output APP module for iterative decoding of concatenated codes," *IEEE Commun. Lett.*, vol. 1, pp. 22-24, Jan. 1997.

[11] M. Xiao and T. Aulin, "Irregular repeat continuous phase modulation," *IEEE Commun. Lett.*, vol. 9, pp. 723-725, Aug. 2005.

[12] S. Cheng, M. C. Valenti, and D. Torrieri, "Coherent and multi-symbol noncoherent CPFSK: capacity and code design," in *Proc. IEEE Military Commun. Conf. (MILCOM)*, Orlando, FL, Oct. 2007.

[13] X. Li and J. A. Ritcey, "Bit-interleaved coded modulation with iterative decoding using soft feedback," *Electron. Lett.*, vol. 34, pp. 942-943, May 14, 1998.

[14] A. J. Viterbi, "An intuitive justification and a simplified implemetation of the MAP decoder for convolutional codes," *IEEE J. Sel. Areas Commun.*, vol. 16, pp. 260-264, Feb. 1998.

[15] E. K. Hall and S. G. Wilson, "Turbo codes for noncoherent channels," in *Proc. IEEE GLOBECOM, Commun. Theory Mini-Conf.*, Phoenix, AZ, pp. 66-70, Nov. 1997.

[16] J. G. Proakis and M. Salehi, *Digital Communications*, 5th edition. New York: McGraw-Hill, Inc., 2008.

[17] European Telecommunications Standards Institute, "Universal mobile telecommunications system (UMTS): multiplexing and channel coding (FDD)," 3GPP TS 25.212 version 3.4.0, Sep. 23, 2000.

Matthew C. Valenti is a Professor in the Lane Department of Computer Science and Electrical Engineering at West Virginia University. He holds BS and Ph.D. degrees in Electrical Engineering from Virginia Tech and a MS in Electrical Engineering from the Johns Hopkins University. From 1992 to 1995 he was an electronics engineer at the US Naval Research Laboratory. He serves as an associate editor for IEEE Transactions on Wireless Communications, and has served as a track or symposium co-chair for the Fall 2007 VTC, ICC-2009, Milcom-2010, and ICC-2011. His research interests are in the areas of communication theory, error correction coding, applied information theory, wireless networks, simulation, and grid computing. His research is funded by the NSF and DoD.

Shi Cheng received the B.E. and M.S. degrees in electrical engineering from Southeast University, Nanjing, China in 2000 and 2003 respectively, and the Ph.D. degree in electrical engineering from West Virginia Unversity, Morgantown, WV in 2007. He is currently a principal engineer in Applied Micro Circuits Corporation, Sunnyvale, CA. His research interests lie in the areas of information theory, coding theory, and communications signal processing.

Don Torrieri is a research engineer and Fellow of the US Army Research Laboratory. His primary research interests are communication systems, adaptive arrays, and signal processing. He received the Ph. D. degree from the University of Maryland. He is the author of many articles and several books including *Principles of Spread-Spectrum Communication Systems* (Springer, 2005). He teaches graduate courses at Johns Hopkins University and has taught many short courses. In 2004, he received the Military Communications Conference achievement award for sustained contributions to the field.